Pharmaceutical Sciences and Drug Design
ISSN: 3062-4428
2023, Volume 3, Page No: 117-127

Available online at: www.galaxypub.co/page/journals

Galaxy Publication

Galaxy Publication

Population Pharmacokinetics of Sirolimus in Adult Liver Transplant Recipients: Hematocrit-Guided Dosing Recommendations from a Large Cohort

Elena Russo[1]*, Matteo Rossi[1], Nicola Gallo[1]

[1]Department of Biotechnology, Faculty of Science, University of Padua, Padua, Italy.

***E-mail** ✉ elena.russo.it@outlook.com

Received: 23 February 2023; **Revised:** 23 May 2023; **Accepted:** 29 May 2023

ABSTRACT

Sirolimus is widely prescribed as an immunosuppressive agent following solid organ transplantation. Its therapeutic index is narrow and exposure is highly inconsistent across individuals, highlighting the need to clarify the contributors to this variability and create patient-specific dosing strategies. This work sought to conduct a population pharmacokinetic (PK) evaluation of sirolimus in adult recipients of liver transplants and to formulate dosage recommendations tailored to patient-level characteristics. A dataset of 216 whole-blood sirolimus concentration measurements from 103 adult subjects was used. Potential PK-related covariates were assessed through a stepwise selection procedure. Monte Carlo simulations were applied to propose dosage options for patients across different covariate categories.

A one-compartment structure with first-order elimination most accurately described the observations. Hematocrit (HCT) was found to significantly affect sirolimus apparent clearance. Monte Carlo simulations indicated that individuals with a low HCT of 28% should receive 1.5 mg qd or 1 mg qd alternated with 1.5 mg qd. For those with normal HCT values, suggested regimens were 1 mg qd, 2 mg qod, or 0.5 mg qd alternating with 1 mg qd. Drawing from the largest population PK dataset of sirolimus in adult liver transplant patients available so far, we propose HCT-guided dosing regimens for this population.

Keywords: Sirolimus, Population pharmacokinetics, Individualized dosing, Liver transplantation, Hematocrit

How to Cite This Article: Russo E, Rossi M, Gallo N. Population Pharmacokinetics of Sirolimus in Adult Liver Transplant Recipients: Hematocrit-Guided Dosing Recommendations from a Large Cohort. Pharm Sci Drug Des. 2023;3:117-27. https://doi.org/10.51847/ab1Lsk1aJD

Introduction

Sirolimus (rapamycin) is routinely administered after solid organ transplantation to reduce the likelihood of allograft rejection. Its pharmacological activity involves interaction with FK-binding protein-12 (FKBP-12), which then suppresses activation of the mammalian target of rapamycin (mTOR) [1]. This blockade prevents cell-cycle progression from the G1 to S phase [2, 3]. Because of this distinct mechanism, along with strong efficacy and a generally favorable safety pattern, sirolimus has extensive clinical use [4].

Following oral dosing, sirolimus is absorbed efficiently, reaching maximum concentrations between 0.5 and 3 h [5, 6]. It distributes broadly across tissues, with marked accumulation within erythrocytes in whole blood [7]. Metabolism occurs mainly through CYP3A4, CYP3A5, and the P-glycoprotein efflux system, with excretion largely via bile and feces [3, 5, 6].

Substantial between-subject variability (BSV) in sirolimus metabolism has been documented. Research in renal transplant patients shows apparent clearance (CL/F) ranging from 90 to 416 mL/h/kg [8], contributing to notable differences in drug levels despite identical dosing. The therapeutic window is narrow, set at 4–8 ng/mL [9, 10]. Consequently, therapeutic drug monitoring (TDM) of trough concentrations (C_0) is routinely used to adjust doses clinically.

Nevertheless, TDM-based dose modification has inherent restrictions because adjustments are only possible once therapy has started. A population PK model, on the other hand, can characterize typical parameters, explain variability, and support individualized dosing from treatment initiation forward.

Although several population PK investigations of sirolimus exist in adult and pediatric cohorts [11-15], only one prior study has focused on adult liver transplant recipients [10]. Its limited sample size restricts generalization. To address this gap, the present study evaluated the influence of multiple covariates on sirolimus PK in adult liver transplant patients and generated dosing recommendations through model-based simulations.

Materials and Methods

Patient characteristics

This work used a retrospective dataset composed of individuals treated with sirolimus tablets after liver transplantation at Tongji Hospital (Tongji Medical College, Huazhong University of Science and Technology) from January 2018 to August 2024. All transplanted organs originated from voluntary donors who provided written consent, and donation procedures complied with the Declaration of Istanbul. Because the project analyzed existing records, the Tongji Hospital Ethics Committee authorized the study (TJ-IRB202409087) and waived additional informed-consent requirements. The study was also conducted in alignment with the 2013 Declaration of Helsinki.

Information extracted from patient charts covered:

1. Drug administration and sampling details—sirolimus dose patterns, timestamps for each administration and blood draw, TDM-reported sirolimus levels, and total daily dosage;
2. Demographics—postoperative day, age, sex, stature, weight, and BMI;
3. Clinical laboratory indices—hemoglobin, hematocrit (HCT), alanine aminotransferase, aspartate aminotransferase, total protein, albumin, total bilirubin, alkaline phosphatase, γ-glutamyl transpeptidase, blood urea nitrogen, serum creatinine, and creatinine clearance;
4. Concurrent medications—prednisone acetate, mycophenolic acid (MPA), esomeprazole, ganciclovir, Wuzhi capsules (a traditional Chinese preparation used for drug-associated hepatic dysfunction), and amlodipine.

All researchers confirmed that no identifiable personal information was retained in the dataset to safeguard patient privacy.

Concentration measurement

Trough sirolimus levels (C_0) were quantified using an enzyme-multiplied immunoassay on the Architect i1000 Automatic Chemiluminescence Immunoassay Analyzer (Abbott Diagnostics Inc., IL, USA) in combination with the ARCHITECT Sirolimus Reagent Kit. The analytic performance showed intra- and inter-day coefficient variations under 10%. The measurable concentration span was 2–30 ng/mL, with a lower detection capability of 0.3 ng/mL.

Model development

Population modeling was conducted with NONMEM (v7.5, Icon Inc., PA, USA) employing the FOCE-I estimation strategy. Perl-speaks-NONMEM (v5.2.6) supported model construction and diagnostic testing. All statistical treatments and graphic outputs were produced in R v4.2.1.

Base model

The structural framework adopted a one-compartment representation with first-order absorption and elimination. Since only C_0 data were available, the absorption rate constant (Ka) was fixed at 0.75 h^{-1}, in line with earlier publications [10]. Inter-individual variability for pharmacokinetic parameters was expressed through exponential terms (Eq. 1).

$$P_{i=TV(P)}.e^{\eta_i} \quad (1)$$

where P_i denotes the pharmacokinetic estimate for the i-th individual, TV(P) corresponds to the population-typical value of that parameter, and η_i represents the inter-individual random effect, assumed to follow a normal distribution with mean 0 and variance ω^2.

Additive (Eq. 2), proportional (Eq. 3), and mixed (additive plus proportional) error structures (Eq. 4) were tested to account for the residual unexplained variability (RUV).

$$Y = F + \varepsilon_1 \quad (2)$$

$$Y = F + F.\ \varepsilon_1 \quad (3)$$

$$Y = F.(1 + \varepsilon_1) + \varepsilon_2 \quad (4)$$

where Y denotes the experimentally obtained sirolimus level and F indicates the concentration predicted by the model, while ε captures the residual error term, assumed to follow a normal distribution centered at 0 with variance σ^2.

Assessment of the base model relied on several considerations, including the stability of parameter estimates, changes in the objective function value (OFV), the Akaike information criterion [16], the Bayesian information criterion [17], and the overall condition number.

Covariate model

Demographic and laboratory variables were inspected for mutual correlations to prevent collinearity. When two strongly related factors were identified, only one was retained for modeling. The covariates explored included: (1) Continuous factors such as age, daily dose, postoperative day, weight, HCT, alanine aminotransferase, and creatinine clearance;
(2) Categorical factors, including sex and concomitant therapies.

Continuous predictors were rescaled to the population median through a power-based function, expressed in Eq. 5.

$$P_i = TV(P).\left(\frac{COV_i}{COV_{median}}\right)^{\theta} \quad (5)$$

where COV_i represents the continuous covariate value for the ith subject, COV_{median} is the median population value of that covariate, and θ denotes the coefficient describing how that covariate influences the PK parameter. Categorical variables were incorporated via a proportional function, presented in Eq. 6:

$$P_i = TV(P).(1 + \theta.COV) \quad (6)$$

where COV is the categorical factor coded as 0 or 1.

Candidate covariates were screened through forward inclusion and backward removal. A covariate was accepted if its inclusion lowered the OFV by more than 3.84 ($P < 0.05$; df = 1) and retained if deleting it caused the OFV to rise by more than 6.63 ($P < 0.01$; df = 1).

Model evaluation

The final population PK framework was examined using goodness-of-fit (GOF) graphics to determine how closely model-generated values matched the observed data. Parameter robustness was assessed using a nonparametric bootstrap procedure with 1000 replicate samples. A prediction-corrected visual predictive check (pc-VPC) was carried out to evaluate predictive reliability. Normalized prediction distribution error (NPDE) plots were also reviewed to confirm that model residuals followed a normal distribution with mean 0 and variance 1. For clearer visualization, four normalized prediction distribution (NPD) plots were generated in place of NPDE [18].

Dosing regimen recommendation

Using the final population PK framework, Monte Carlo simulations were applied to project steady-state C0 distributions for nine frequently prescribed sirolimus schedules across different covariate profiles. The dosing options examined were: (1) 0.5 mg once daily (qd); (2) 1 mg qd; (3) 1.5 mg qd; (4) 2 mg qd; (5) 1 mg every other day (qod); (6) 2 mg qod; (7) alternating 0.5 mg qd with 1 mg qd; (8) alternating 1 mg qd with 1.5 mg qd; and (9) alternating 1 mg qd with 2 mg qd. Regimen recommendations for individuals with different covariate patterns were selected from the simulated C0 distributions, ensuring the majority of predicted exposures stayed within the therapeutic target of 4–8 ng/mL [9, 10].

Results and Discussion

Patient characteristics

For the PK assessment, 216 whole-blood concentrations from 103 adults were analyzed. All subjects were post–liver transplantation and receiving sirolimus for graft-rejection prevention. Median values for age, body weight, and BMI were 51 years, 68.0 kg, and 23.8 kg/m², respectively. Regimens used in this cohort included: 0.5 mg qd, 1 mg qd, 2 mg qd, 1 mg qod, 2 mg qod, alternating 0.5/1 mg qd, and alternating 1/2 mg qd. Baseline features of the study population are listed in **Table 1**.

Table 1. Baseline Demographic Information for the Population Used in the PK Modeling

Patient Characteristic	Mean ± SD	Median [Range]
Sex (male/female), n	99/4	–
Age (years)	50.4 ± 9.20	51.0 [28.0 – 74.0]
Height (cm)	170 ± 5.40	170 [150 – 183]
Body weight (kg)	68.6 ± 10.2	68.0 [39.0 – 90.0]
Body mass index (kg/m²)	23.6 ± 3.11	23.8 [16.7 – 30.8]
Postoperative days	145 ± 140	92 [14 – 699]
Sirolimus daily dose (mg/day)	1.02 ± 0.32	1.0 [0.5 – 2.0]
Sirolimus trough concentration (ng/mL)	5.45 ± 1.96	5.26 [1.33 – 12.17]
Hemoglobin (g/L)	125 ± 23.7	126 [57 – 168]
Hematocrit (%)	37.8 ± 6.60	38.0 [17.5 – 49.5]
Total serum protein (g/L)	74.2 ± 7.82	74.4 [50.3 – 105.0]
Albumin (g/L)	43.1 ± 4.85	44.2 [27.2 – 50.9]
Alanine aminotransferase (U/L)	38.0 ± 38.5	21.0 [5.0 – 187.0]
Aspartate aminotransferase (U/L)	37.1 ± 32.7	25.0 [12.0 – 190.0]
Alkaline phosphatase (U/L)	145 ± 131	104 [8 – 1040]
γ-Glutamyl transpeptidase (U/L)	109 ± 170	58.0 [13.0 – 1110]
Total bilirubin (μmol/L)	22.5 ± 32.3	53.55 [2.50 – 308.0]
Blood urea nitrogen (mmol/L)	7.22 ± 5.14	6.07 [2.4 – 38.7]
Serum creatinine (μmol/L)	94.6 ± 40.7	81.0 [49.0 – 267.0]
Creatinine clearance (mL/min)[a]	88.9 ± 30.4	89.4 [27.0 – 170.0]
Concomitant medications (with/without), n		
Ganciclovir	5/98	
Prednisone acetate	10/93	
Esomeprazole	10/93	
Amlodipine	10/93	
Mycophenolic acid	24/79	
Wuzhi capsule	26/77	

Note: aCreatinine clearance was estimated via the Cockcroft–Gault equation:
creati- nine clearance = [140 – age (years)] × weight (kg) / [0.818 × SCR (μmol/L)] × k, where k = 1 for males and 0.85 for females.
Abbreviation: SD = standard deviation.

Model development

A single-compartment structure with first-order elimination most adequately represented the concentration-time profiles. Between-subject variability (BSV) was quantified for CL/F and V/F. A mixed residual-error structure was used to capture RUV, and a correlation term between CL/F and V/F was estimated.

Introducing HCT into the clearance model produced a statistically meaningful drop in OFV (32.9). None of the covariates were excluded during backward elimination (P > 0.01), leaving HCT as the only retained covariate in the final specification. The completed population PK model is shown below (Eqs. 7–9):

$$K_a(h^{-1}) = 0.75 \quad (7)$$

$$CL/F(L/H) = 7.09 \times \left(\frac{HCT}{38}\right)^{-0.901} \quad (8)$$

$$V/F(L) = 496 \quad (9)$$

Parameter estimates and bootstrap summaries are listed in **Table 2**, with all relative standard errors remaining below 30%, demonstrating acceptable precision.

Table 2. Final Model Parameter Estimates and Bootstrap Outputs

Parameter	Final Model Estimate	RSE (%)	Bootstrap Median	Bootstrap 95% CI (2.5th–97.5th percentile)
Fixed effects				
ka (h^{-1})	0.75	Fixed	–	–
CL/F (L/h)	7.09	4	7.02	6.44 – 7.59
V/F (L)	496	15	515.85	306.28 – 687.11
Effect of HCT on CL/F (exponent)	−0.901	17	−0.873	−1.259 – −0.551
Inter-individual variability				
ω² CL/F (%)	32.4	9	31.9	25.1 – 37.9
ω² V/F (%)	42.7	19	40.1	17.7 – 59.2
Covariance ω_(CL/F,V/F)	0.0665	–	0.0695	0.0062 – 0.1317
Residual variability				
Proportional error ε_por (%)	3.3	10	3.19	2.41 – 3.81

Abbreviations: CL/F = apparent clearance (L/h); HCT = hematocrit (%); k_a = absorption rate constant (h^{-1}); V/F = apparent central distribution volume (L); RSE = relative standard error; $\omega_{CL/F}$= BSV for clearance; $\omega_{V/F}$= BSV for V/F; ε_{por}= proportional residual variability.

Model evaluation

Goodness-of-fit diagnostics indicated appropriate model performance **(Figure 1)**. Observed concentrations aligned well with both individual and population predictions, with points symmetrically positioned around the identity line **(Figures 1a and 1b)**. Conditional weighted residuals were predominantly centered near zero and mostly within ±2 **(Figures 1c and 1d)**.

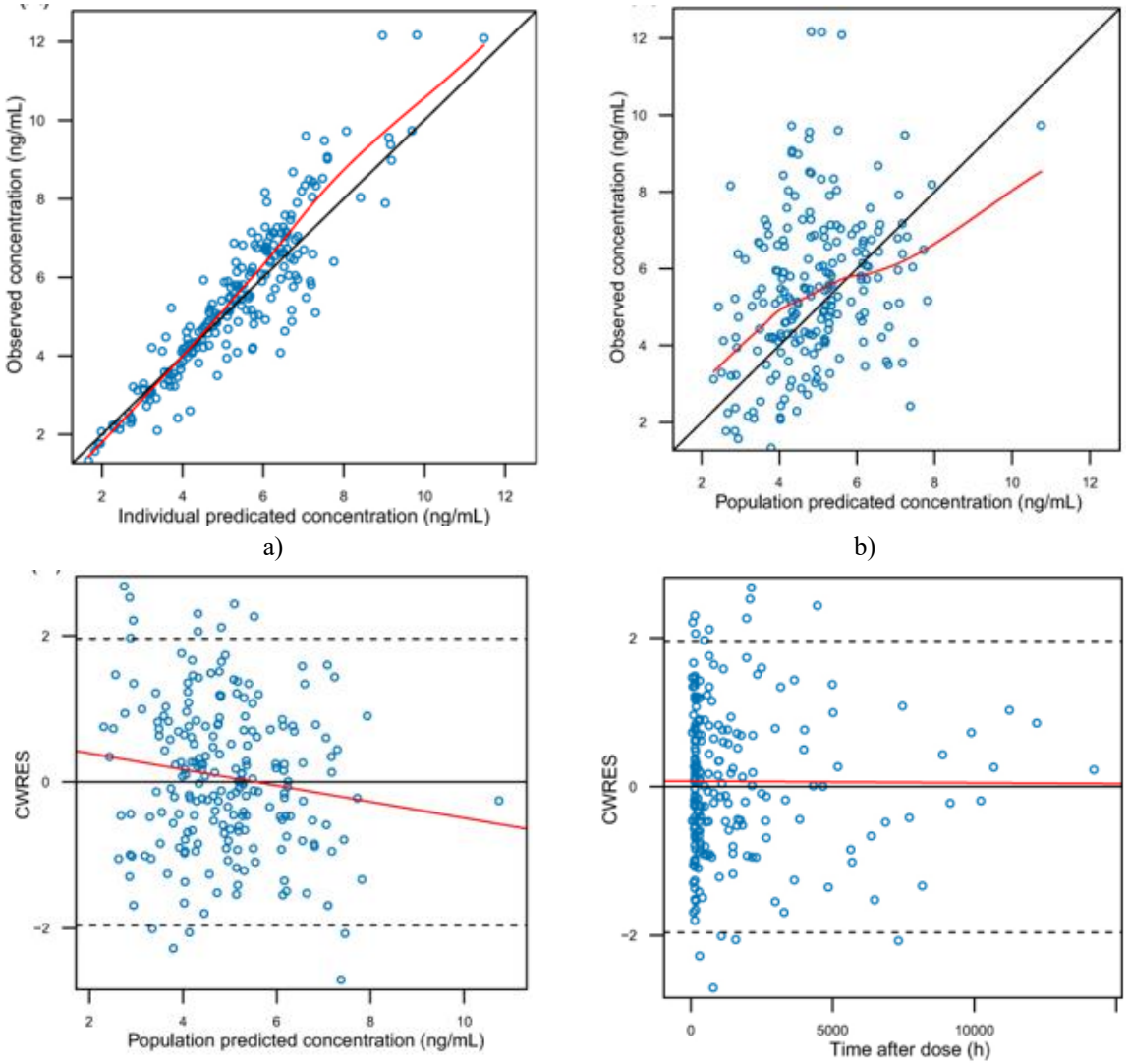

Figure 1. Goodness-of-Fit Assessments for the Final Model.
(a) Observed vs individual predictions; (b) observed vs population predictions (PRED); (C) CWRES vs PRED; (D) CWRES vs time post-dose. Black lines correspond to identity references; red curves represent loess smoothing.

Bootstrap analysis

Out of the 1000 bootstrap replicates, 97.5% completed without failure. The estimated parameters from the finalized model fell entirely within the corresponding bootstrap-derived 95% confidence intervals (CI), confirming the stability of the model outputs **(Table 2)**.

The prediction-corrected VPC (pc-VPC) also showed strong concordance between simulated and empirical concentrations **(Figure 2)**. The 5th, 50th, and 95th percentiles of the observed data generally aligned with the simulated 90% CIs.

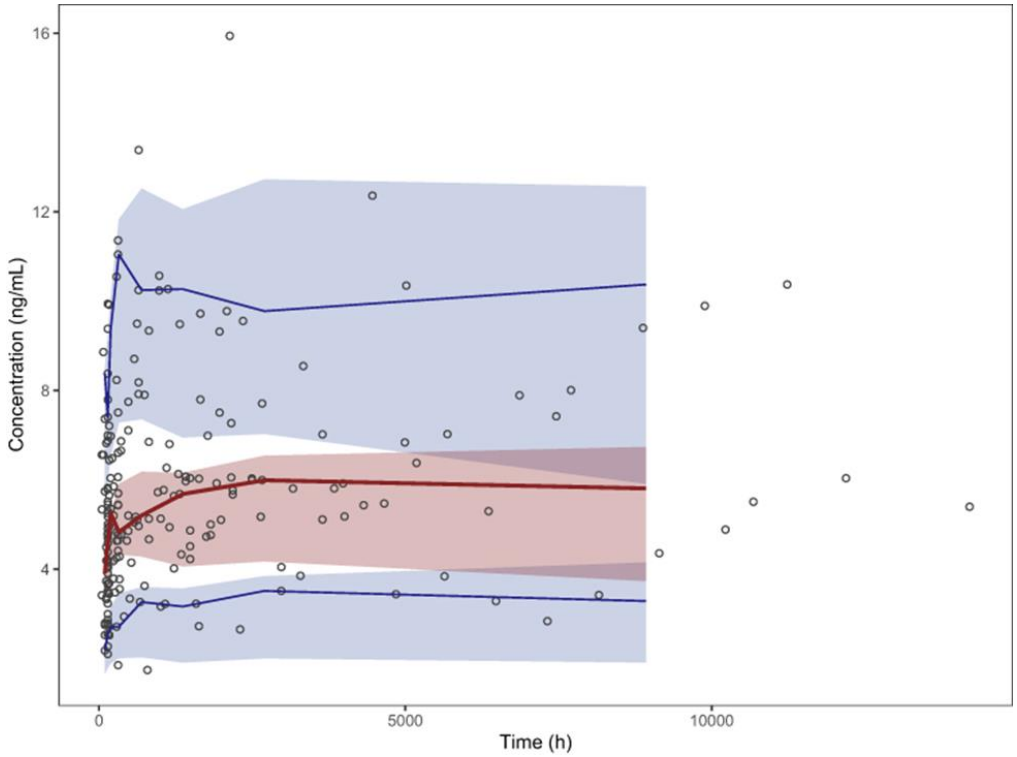

Figure 2. Prediction-corrected VPC for the final PK model. Dots indicate measured concentrations; solid curves display the median (red) and the 5th/95th percentiles (blue) of observations. Shaded regions denote the 90% CIs of the simulated median (red) and the simulated 5th/95th percentiles (blue).

No systematic deviations were apparent in the NPD diagnostics **(Figures 3a–3d)**. The Wilcoxon signed-rank test, Fisher's variance test, the Shapiro–Wilk test, and the global assessment all returned P values > 0.5, indicating that the model adequately captured the underlying data.

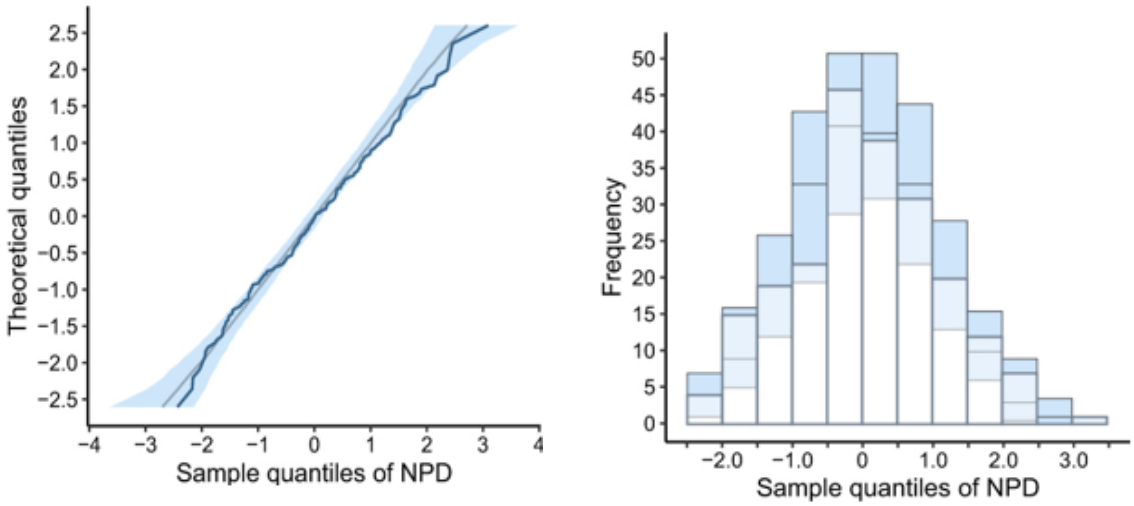

a) b)

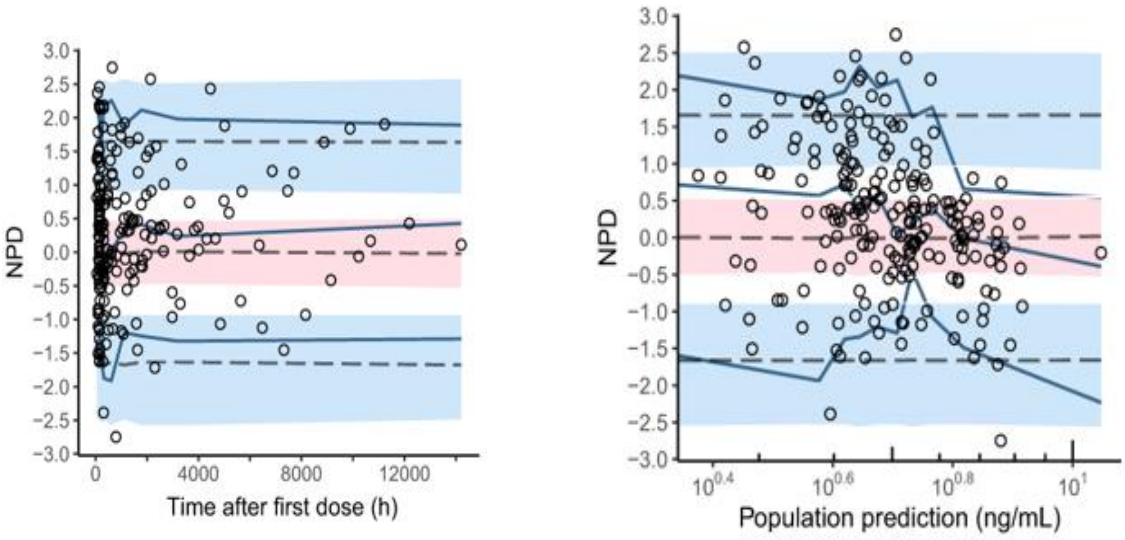

c) d)

Figure 3. Normalized prediction distribution (NPD) diagnostics. (a) Q–Q comparison of NPD values with a theoretical normal distribution; (b) histogram of NPD values with standard normal density overlay; (c) NPD plotted against time following the first administration; (d) NPD versus population-predicted concentrations.

Dosing regimen recommendation

Since HCT was identified as a covariate in the final PK structure, steady-state C0 levels were simulated for all nine sirolimus regimens using HCT values fixed at the 10th, 50th, and 90th percentiles of the study population: 28%, 38%, and 46%. The resulting C0 distributions are illustrated in **Figure 4**.

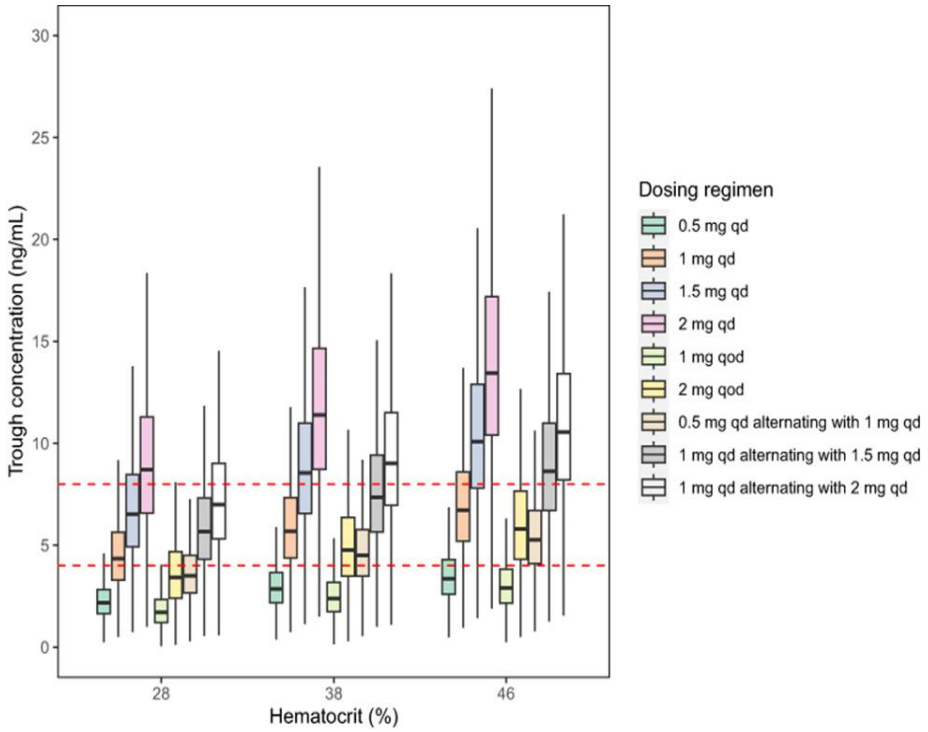

Figure 4. Boxplots of simulated steady-state trough concentrations for sirolimus at HCT levels of 28%, 38%, and 46%. The dashed horizontal boundaries mark the therapeutic interval of 4–8 ng/mL.

Monte Carlo outcomes indicated that higher HCT was associated with a reduced daily requirement for maintaining concentrations within the therapeutic target, assuming the same dosing frequency. For individuals with a low HCT of 28%, suggested regimens include 1.5 mg qd or alternating 1 mg qd with 1.5 mg qd. For those with HCT values of 38% or 46%, appropriate options include 1 mg qd, 2 mg qod, or alternating 0.5 mg qd with 1 mg qd.

To our knowledge, this work presents the largest dataset thus far for constructing a population PK model of sirolimus in individuals undergoing liver transplantation. A single-compartment framework with first-order elimination was sufficient to characterize sirolimus disposition. In addition, model-based evaluations allowed us to propose several dosing strategies for patients exhibiting different HCT values.

The PK estimates generated from sparse sampling were in line with previously published reports. Zhang *et al*. [10] documented a CL/F of 6.97 L/h and a V/F of 457.85 L in adult hepatic transplant recipients, figures comparable to ours (CL/F: 7.09 L/h; V/F: 496 L). Previous population PK assessments have also been conducted in other transplant groups, such as those receiving renal grafts [14, 19–21] or heart transplants [15]. Our calculated CL/F matched that reported for heart transplant patients,15 yet it fell slightly below the 8.91–14.4 L/h range described for renal transplant recipients [19, 21]. This discrepancy may relate to the substantial hepatic CYP3A-mediated biotransformation of sirolimus. Moreover, incomplete recovery of grafted liver function could partially explain the reduced CL/F observed in liver transplant patients.

With respect to V/F, our value was within the 322–727 L range noted for renal transplant cohorts [20, 21], but still far lower than the 1350 L reported for heart transplant recipients [15]. This variation may be attributed to reliance solely on C0 samples, which limits accurate V/F estimation.

HCT emerged as the only significant covariate influencing CL/F in the final model. Higher HCT corresponded to reduced CL/F, consistent with findings in individuals with advanced malignancies [22]. Since approximately 95% of sirolimus partitions into erythrocytes [23], elevated HCT likely decreases the free fraction, resulting in diminished clearance.

We also examined the impact of concurrent medications on sirolimus kinetics. During forward inclusion, MPA and Wuzhi capsules were retained as binary covariates; however, they were later excluded in the backward elimination step because their effects were not statistically meaningful and their coefficients were imprecisely estimated.

Wuzhi capsules act as strong CYP3A4 inhibitors [24]. Given that CYP3A4 is the principal metabolic pathway for sirolimus, coadministration of CYP3A4 inhibitors could alter its metabolism. Additionally, a pharmacokinetic interaction between MPA and sirolimus is possible. Dösch *et al*. [25] observed that dose-normalized MPA C0 values were reduced in the sirolimus/MPA group compared with the cyclosporin A/MPA group. Thus, further investigations incorporating more detailed co-medication records are needed to refine sirolimus dosing.

In real-world settings, sirolimus dosing for liver transplant adults is often intricate because of its narrow therapeutic index. Our simulation results showed that when HCT levels were within normal limits, an extended dosing interval—specifically, every other day—could be considered. This is likely due to sirolimus's long elimination half-life (62 h), which helps maintain C0 within target limits. A well-adjusted regimen may minimize the frequency of dose modifications and lower the risk of toxicity due to overexposure.

This study has limitations. First, only trough samples were collected, leading to a fixed Ka and less robust V/F estimation; future prospective studies should explore the absorption and distribution phases more comprehensively. Second, despite representing the largest dataset of sirolimus concentrations in adult liver transplant recipients, the sample was still insufficient to thoroughly assess the effect of co-administered therapies on sirolimus PK. Third, because all measurements originated from a single institution, external validation is necessary to confirm the generalizability of this model.

Conclusion

In summary, we established a population PK model of sirolimus in adult liver transplant patients using the largest dataset reported so far. HCT was confirmed as a key determinant of sirolimus CL/F. Tailored dosing should be considered across nine commonly used regimens to accommodate varying HCT levels.

Acknowledgments: None

Conflict of Interest: None

Financial Support: None

Ethics Statement: None

References

1. Sehgal S. Sirolimus: a new immunosuppressive agent: a historical perspective and immunosuppressive profile. In: Principles of Drug Development in Transplantation and Autoimmunity. Austin, TX: RG Landes; 1996:271–82.
2. Stenton SB, Partovi N, Ensom MH. Sirolimus: the evidence for clinical pharmacokinetic monitoring. Clin Pharmacokinet. 2005;44(8):769–86. doi:10.2165/00003088-200544080-00001
3. MacDonald A, Scarola J, Burke JT, Zimmerman JJ. Clinical pharmacokinetics and therapeutic drug monitoring of sirolimus. Clin Ther. 2000;22(Suppl B):B101–21. doi:10.1016/s0149-2918(00)89027-x
4. Sehgal SN. Sirolimus: its discovery, biological properties, and mechanism of action. Transplant Proc. 2003;35(3 Suppl):7s–14s. doi:10.1016/s0041-1345(03)00211-2
5. Mahalati K, Kahan BD. Clinical pharmacokinetics of sirolimus. Clin Pharmacokinet. 2001;40(8):573–85. doi:10.2165/00003088-200140080-00002
6. Augustine JJ, Bodziak KA, Hricik DE. Use of sirolimus in solid organ transplantation. Drugs. 2007;67(3):369–91. doi:10.2165/00003495-200767030-00004
7. Meier-Kriesche HU, Kaplan B. Toxicity and efficacy of sirolimus: relationship to whole-blood concentrations. Clin Ther. 2000;22(Suppl B):B93–100. doi:10.1016/s0149-2918(00)89026-8
8. Zimmerman JJ, Kahan BD. Pharmacokinetics of sirolimus in stable renal transplant patients after multiple oral dose administration. J Clin Pharmacol. 1997;37(5):405–15. doi:10.1002/j.1552-4604.1997.tb04318.x
9. Masters JC, Shah MM, Feist AA. Drug interaction between sirolimus and ranolazine in a kidney transplant patient. Case Rep Transplant. 2014;2014:548243. doi:10.1155/2014/548243
10. Zhang Y, Zhang X, Zou Y, Sun Y, Li X. Population pharmacokinetics of sirolimus in Chinese adult liver transplant recipients: a retrospective study. Xenobiotica. 2021;51(12):1408–15. doi:10.1080/00498254.2022.2025628
11. Shen G, Moua KT, Perkins K, Johnson D, Li A, Curtin P, et al. Precision sirolimus dosing in children: the potential for model-informed dosing and novel drug monitoring. Front Pharmacol. 2023;14:1126981. doi:10.3389/fphar.2023.1126981
12. Li S, Zhan M, Wu S, Liao J, Xu H, Sun D, et al. Population pharmacokinetic analysis and dosing optimization of sirolimus in children with tuberous sclerosis complex. J Clin Pharmacol. 2022;62(8):948–59. doi:10.1002/jcph.2033
13. Liu B, Zhang X, Zhao Y, Xu X, Wang S, Wang X, et al. Model-Informed individualized dosage regimen of sirolimus in pediatric patients with intractable lymphatic malformations. Eur J Pharm Sci. 2024;200:106837. doi:10.1016/j.ejps.2024.106837
14. Djebli N, Rousseau A, Hoizey G, Rerolle JP, Toupance O, Le Meur Y, et al. Sirolimus population pharmacokinetic/pharmacogenetic analysis and Bayesian modelling in kidney transplant recipients. Clin Pharmacokinet. 2006;45(11):1135–48. doi:10.2165/00003088-200645110-00007
15. Zahir H, Keogh AM, Akhlaghi F. Apparent clearance of sirolimus in heart transplant recipients: impact of primary diagnosis and serum lipids. Ther Drug Monit. 2006;28(5):614–22. doi:10.1097/01.ftd.0000246765.05248.fa
16. Yamaoka K, Nakagawa T, Uno T. Application of Akaike's information criterion (AIC) in the evaluation of linear pharmacokinetic equations. J Pharmacokinet Biopharm. 1978;6(2):165–75. doi:10.1007/bf01117450
17. Vrieze SI. Model selection and psychological theory: a discussion of the differences between the Akaike information criterion (AIC) and the Bayesian information criterion (BIC). Psychol Methods. 2012;17(2):228–43. doi:10.1037/a0027127
18. Nguyen TH, Mouksassi MS, Holford N, Al-Huniti N, Freedman I, Hooker AC, et al. Model evaluation of continuous data pharmacometric models: metrics and graphics. CPT Pharmacometrics Syst Pharmacol. 2017;6(2):87–109. doi:10.1002/psp4.12161
19. Ferron GM, Mishina EV, Zimmerman JJ, Jusko WJ. Population pharmacokinetics of sirolimus in kidney transplant patients. Clin Pharmacol Ther. 1997;61(4):416–28. doi:10.1016/s0009-9236(97)90192-2
20. Golubović B, Vučićević K, Radivojević D, Kovačević SV, Prostran M, Miljković B. Exploring sirolimus pharmacokinetic variability using data available from the routine clinical care of renal transplant patients - population pharmacokinetic approach. J Med Biochem. 2019;38(3):323–31. doi:10.2478/jomb-2018-0030

21. Shi HQ, Yang J, Zhang LQ, Xu BM, Lu HL, Chen EZ, et al. The population pharmacokinetics of sirolimus and CYP3A5*3 polymorphism in Chinese renal transplant patients. Int J Clin Exp Med. 2016;9(3):5854–66.
22. Wu K, Cohen EE, House LK, Ramírez J, Zhang W, Ratain MJ, et al. Nonlinear population pharmacokinetics of sirolimus in patients with advanced cancer. CPT Pharmacometrics Syst Pharmacol. 2012;1(12):e17. doi:10.1038/psp.2012.18
23. Methaneethorn J, Art-Arsa P, Kosiyaporn R, Leelakanok N. Predictors of sirolimus pharmacokinetic variability identified using a nonlinear mixed effects approach: a systematic review. J Popul Ther Clin Pharmacol. 2022;29(4):e11–e29. doi:10.47750/jptcp.2022.940
24. Li ZR, Li RD, Niu WJ, Zheng XY, Wang ZX, Zhong MK, et al. Population pharmacokinetic modeling combined with machine learning approach improved tacrolimus trough concentration prediction in Chinese adult liver transplant recipients. J Clin Pharmacol. 2023;63(3):314–25. doi:10.1002/jcph.2156
25. Dösch AO, Ehlermann P, Koch A, Remppis A, Katus HA, Dengler TJ. A comparison of measured trough levels and abbreviated AUC estimation by limited sampling strategies for monitoring mycophenolic acid exposure in stable heart transplant patients receiving cyclosporin A-containing and cyclosporin A-free immunosuppressive regimens. Clin Ther. 2006;28(6):893–905. doi:10.1016/j.clinthera.2006.06.015